International Journal of Engineering

Journal Homepage: www.ije.ir

Synthesis of Hard Layer by Titanium Addition During Welding Process and Quenched Directly

S. Syaripuddin*[a], S. Sopiyan[a], S. Aditya[a], S. D. Yudanto[b], F. B. Susetyo[a]

[a] *Department of Mechanical Engineering, Universitas Negeri Jakarta, Jakarta, Indonesia*
[b] *Research Center for Metallurgy - National Research and Innovation Agency, Serpong, Indonesia*

PAPER INFO

Paper history:
Received 02 December 2022
Received in revised form 31 December 2022
Accepted 01 January 2023

Keywords:
Hardfacing
Ti
Welding
Hardness
Quenching Oil

ABSTRACT

Enhance the surface hardness of materials usually conducted through a hardfacing technique. Hardfacing is popular, whereby materials with better properties are deposited over cheaper bulk material. This work fabricated hard layers by adding titanium (Ti) wire during the welding process. This research used low-carbon steel as the base material, wire optime Ti grade 1 for Ti addition, and an HV 600 electrode with a diameter of 3.2 mm for filler metal. A single-layer weld was conducted with SMAW (positive polarity and 90 A). The samples were directly quenched in a different solution after welding. The properties of the weld layer were examined phase, structure, microstructure, macrostructure, and hardness using optical emission spectroscopy (OES), x-ray diffraction (XRD), an optical microscope, a digital camera, and a hardness device, respectively. Adding titanium (Ti) to the weld layer and quenching the samples after welding in the solution enhances the hardness. This phenomenon is attributed to different phase compositions, oxides, and microstructures. A fine dispersion of small particles and oxide amount is important in increasing hardness. There is no cracking in the weld and base metal. In conclusion, samples BNTiO and BNTiM are recommended for lathe-cutting tools.

***doi**: 10.5829/ije.2023.36.03c.13*

1. INTRODUCTION

High Speed Steel (HSS) is a commonly used cutting tool in the lathe. For dry-cutting operational conditions, four factors need consideration: pressure, temperature, sliding speed, and the interface. Thus, factors could affect high wear rate, heat, and short tool life [1]. These conditions could be reduced by increasing the hardness. HSS commercial lathe-cutting tool hardness is around 765.68 HV [2].

Enhance the surface hardness of materials usually conducted through a hardfacing technique. Hardfacing is popular, whereby materials with better properties are deposited over cheaper bulk material [3]. Furthermore, hardfacing is one of the most economical techniques to mitigate the wear of tools and components of a machine [4]. By increased the hardness on the surface of the metal with less hardness is the cheapest than using a bulk metal with high hardness. Hardfacing applies a hard surface layer on the base material to resist abrasion, impact, and erosion.

Welding is one technique for fusion between two materials [5]. The welding process also could be conducted to reach the hard layer. Therefore, a hard layer could result from welding processes such as shielded metal arc welding (SMAW) [6, 7], Flux core arc welding (FCAW) [6], plasma transferred arc welding (PTA) [8], electro-slag welding (ESW) [9], and gas tungsten arc welding (GTAW) [10]. The SMAW technique is more flexible and easy to operate than others.

Commonly filler metals used for hardfacing are iron (Fe)-based alloys, cobalt (Co)-based alloys, and nickel (Ni)-based alloys. Singh [11] has reported hardfacing single layers through various hard alloy filler metals (iron (Fe)-based alloys), resulting in hardness between 375 and 543 HV. A different electrode composition has resulted in different hardness. A filler metal with a high carbon (C), Manganese (Mn), and chromium (Cr) has a resulting

*Corresponding Author Institutional Email: *Syaripuddin_andre@unj.ac.id* (S. Syaripuddin)

Please cite this article as: S. Syaripuddin, S. Sopiyan, S. Aditya, S. D. Yudanto, F. B. Susetyo, Synthesis of Hard Layer by Titanium Addition During Welding Process and Quenched Directly, ***International Journal of Engineering, Transactions C: Aspects,*** Vol. 36, No. 03, (2023) 532-539

high hardness. Deng et al. [12] reported that hardfacing by cobalt (Co)-based alloys resulted in different hardness for different thicknesses. Less thickness is resulting high hardness. This phenomena is caused by the absence of the fine grain when the thickness is decreased. Kesavan and Kamaraj [8] have found that aging treatment of a nickel-based hardfacing has reduced the hardness when treatment time increased.

Titanium (Ti) and Ti-alloys are widely applied in marine, petrochemical, chemical, aerospace, and biomedical industries because promising high specific strength and high corrosion resistance [13, 14]. Furthermore, Ti also promises good hardness and erosion resistance [15]. Therefore adding a Ti into the weld layer could increase the hardness. Zhou et al. [16] have added 0.263 wt% Ti in the flux of the SMAW filler metal (Fe-Cr13-C-Nb). Exhibit Ti leads to a decreasing hardness from 46.2 to 45.2 HRC. Ti could be aglomerated perfectly between filler and based metal because the flux is changed into gasses as shielding for molten metal when the SMAW process is performed. Zhou et al. [16] found that the hardness of the layer increased from 56 to 61 HRC with titanium content from 0 to 0.63 wt%. Increased Ti content to 1.17 wt% could form TiC carbide because too much carbon is consumed by titanium. It led to a change in the microstructure to a hypereutectoid one and caused a decrease in the hardness. Moreover, the exhibit Ti content in the layer also increases the hardness than Zr addition by approximately 603 and 584 HV, respectively [17].

In addition, increasing the hardness of a material can also be conducted by quenching techniques in various solutions such as oil [18, 19]. Vegetables and engine oil were used for quenching operations to avoid undesirable microstructure [18, 20]. Dauda et al. [20] quenched carbon steel in engine oil, and Totten et al. [21] also quenched steel in vegetable oil which could increase the hardness. Various oils for quenching solution would be resulting different microstructures due to different cooling rates. Engine oil and vegetable oil at 40 ºC have a cooling rate of 64.4 and 71.9 K/s, respectively [21]. The cooling rate decreases as the viscosity of the solution increases [22].

Before quenching, the sample was heated in a muffle furnace. Commonly, the muffle furnace temperature is set to > 800ºC, and the specimen was heated 0.5 until 1 hour [18]. For cost efficiency, the sample quench after the welding process is similar to when the sample heating with a muffle furnace and then rapidly quenching because the temperature during the welding process is around 1200 ºC, which is similar to heating with a muffle furnace [23].

In this research, the hardfacing by the commercial electrode and adding Ti during welding on the low-carbon steel was conducted. Moreover, after welding, each sample was directly quenched in vegetable oil and engine oil. It is worth to be mentioned and to highlight the major concern about properties and hardness result by adding Ti in the weld layer and directly quenching method after weld. This method is more cost-effective than heating the sample with a muffle furnace. The application of this research is for lathe cutting tools application.

2. MATERIALS AND METHODS

This research used low-carbon steel (150×10×10 mm) as the base material. The composition of the base material is 0.128 wt% C, 0.359 wt% Si, 0.996 wt% Mn, 0.225 wt% Cr, 0.167 wt% Cu, and Fe balance (see Figure 1). Wire optime Ti grade 1 with a diameter of 0.65 mm (from the USA) was used for Ti addition. The weight of each Ti wire used is 0.225 g. HV 600 electrode (typical composition: 0.6 wt% C, 1 wt% Mn, 0.4 wt% Si, 4wt% Cr, and Fe balance) with a diameter of 3.2 mm (from Nikko Steel Manufacturer) was used for filler metal.

Prior welding process, the based material surface was cleaned by hand grinder. HV 600 electrode was dried for 1 hour (150 ºC). Three pieces of Ti wire (150×∅ 0.65mm) were placed on the surface of low carbon steel and welded single layer with SMAW (Fro BF 443, positive polarity, and 90 A).

This research was resulting three different samples that were welded using an HV 600 electrode without Ti addition and directly cooled in the natural air, quenched in 1L of engine oil (SAE 20-50), and 1 L of palm oil, namely BNU, BNO, BNM, respectively. Afterward, three samples were welded using an HV 600 with Ti addition. They directly cooled in the natural air, quenched in 1 L of palm oil, and 1L of engine oil (SAE 20-50) were BNTiU, BNTiO, and BNTiU, respectively. The sample after the weld is shown in Figure 2.

The samples were checked with Was Foundry Master-Optical Emission Spectroscopy (OES) according to ASTM E415. X-ray diffraction (XRD) PANalytical Aeris with CoK=1.789 Å and step size 0.0217° was used to analyze the phase composition and crystal structure. The Rietveld method was used to calculate the lattice parameters [24]. Furthermore, the sample was mounted in the epoxy resin, grinding, polishing, etching in 3%

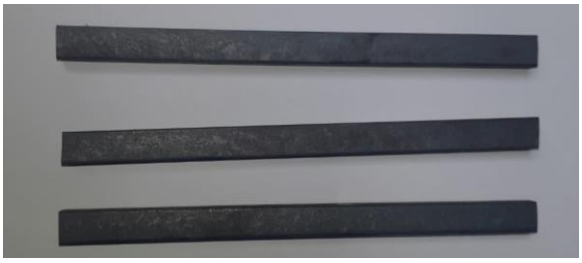

Figure 1. Base material

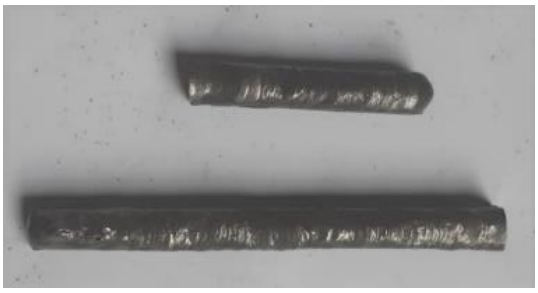

Figure 2. Weld samples

Nital, and captured by a digital camera for macrostructure. It was also checked by an inverted optical metallurgy microscope Olympus BX41M – LED for microstructure investigation (ASTM E407). Afterward, samples were hardness measured by Vickers hardness tester FV-300e (5kg_f of load). Five readings were collected to have average hardness.

3. RESULT AND DISCUSSION

3. 1. OES Based on the OES result, the base material was welded with HV 600 electrodes, resulting welded layer in the composition: 0.342 wt%C, 0.182 wt%Si, 0.608 wt%Mn, 2.09 wt%Cr, 0.139 wt%Cu, and Fe balance. The 0.342 wt%C in the steel is close to medium carbon steel [25].

The base material was welded with HV 600 electrode and added a Ti wire resulting welded layer in the composition: 0.443 wt%C, 0.366 wt%Si, 0.923 wt%Mn, 2.19 wt%Cr, 0.144 wt%Cu, 0.147 wt% Ti, and Fe balance. Ti was perfect adding in the weld layer, as proved by the OES result.

3. 2. XRD Figure 3 shows the diffraction pattern of the various samples. The plane peaks (110) and (211) are reflections of the α-iron (ferrite) phase. These α-iron phase plane peaks are in good agreement with the results of other studies [26-28]. The peak magnification of 110 plane diffraction patterns in the inset of Figure 3 (2θ = 50-53°) shows an asymmetric peak shape. According to Han et al. [28], this asymmetrical peak denotes the presence of an α'-iron (martensite) phase. The peak at an angle of 2θ = 41.3°, identified as the Fe_3O_4 phase, illustrates how the welding process used results in the oxidation of the steel.

Different intensity values can be seen in the diffraction patterns of the four samples. This intensity value can be connected to the full width at half maximum (FWHM) value of each sample. The BNTiO sample has the smallest crystallite size, according to the qualitative analysis of the FWHM values of the α-iron and α'-iron phases in the (110) and (211) planes, as summarized in Table 1.

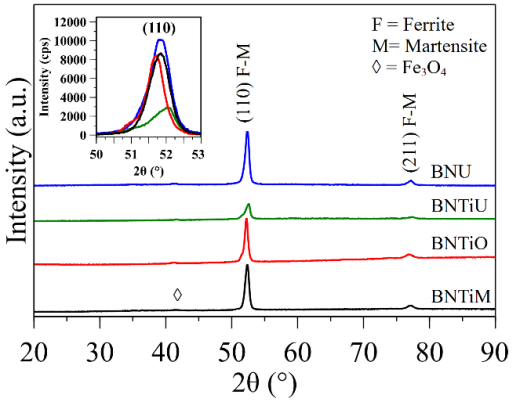

Figure 3. XRD various samples

TABLE 1. Quantitative analysis of diffraction patterns for various samples

Source	BNU	BNTiU	BNTiO	BNTiM
Ferrite phase				
Crystal system: Body Center Cubic (BCC)				
Space group: Im-3m				
Lattice a (nm)	0.2878	0.2867	0.2881	0.2875
Martensite phase				
Crystal system: Body Center Tetragonal (BCT)				
Space group: I4/mmm				
Lattice a (nm)	0.2855	0.2857	0.2859	0.2821
Lattice c (nm)	0.2935	0.2958	0.2931	0.2876
α-Fe (wt.%)	81.24	60.35	72.75	85.41
α'-Fe (wt.%)	15.99	32.30	23.86	13.02
Fe_3O_4 (wt.%)	2.77	7.35	3.39	1.57
FWHM (110) (°)	0.695	0.858	0.548	0.680
FWHM (211) (°)	0.980	1.090	1.030	1.120
Rwp (%)	3.30	5.31	3.46	3.52
χ^2	1.360	1.369	1.662	1.268

The composition of the phase formed and lattice constants were determined through the quantitative analysis of the diffraction patterns. Figure 4 compares the results of the calculated and observed diffraction patterns for the BNTiM sample. This study uses the Rietveld method to analyze diffraction patterns quantitatively. The overlapping peak (110) of the ferrite and martensite phase fractions were calculated using the Rietveld method in order to determine its composition. The ferrite and martensite phase fractions for the BNTiM sample were 85.41 wt.% and 13.02 wt.%, respectively (see Table 1). The sample with the greatest α-iron phase content out of the other three is the BNTiM sample.

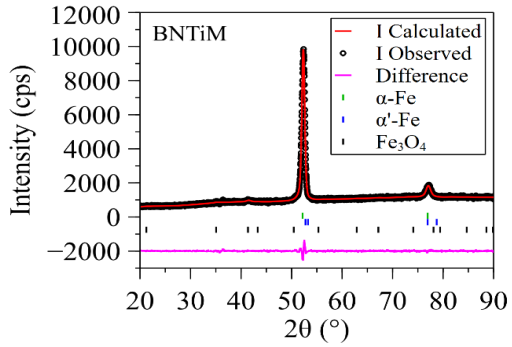

Figure 4. Diffraction patterns for the BNTiM sample calculated with the Rietveld method

The BNTiM sample, which has a body center cubic (BCC) structure with the space group Im-3m, has a lattice constant value (a=b=c) of 0.2875 nm. Table 1 shows the lattice constants for the four samples. These constant lattice values are identical to those previously reported [29-31].

3. 3. Microstructure Microstructure observation for the samples with an optical microscope was conducted as shown in Figure 5.

Based on Figure 5, we can observe different microstructures were formed. Samples with air cooling have similar characteristics for Ti addition and without Ti addition. It seems 0.147 wt% Ti addition does not influence the microstructure. This phenomenon is due to

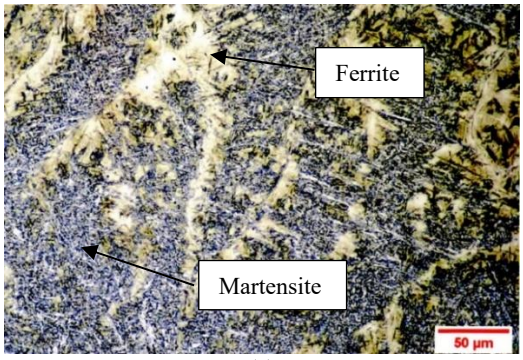

(a)

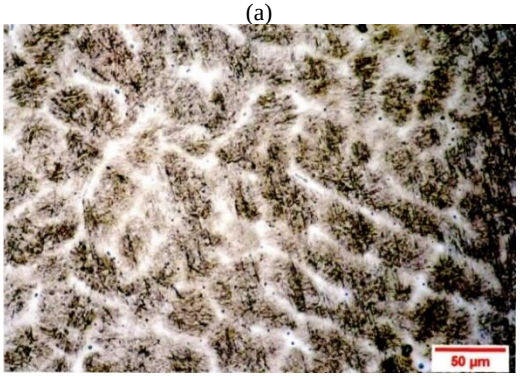

(b)

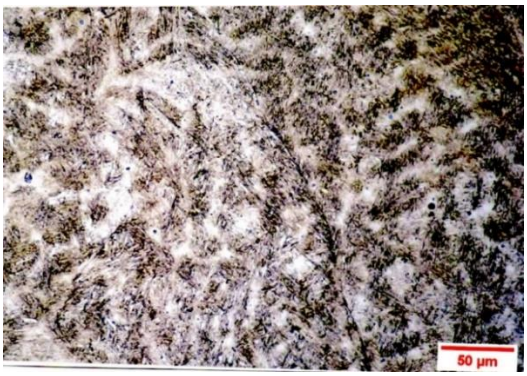

(c)

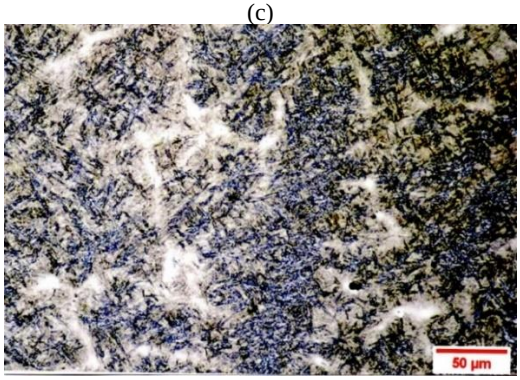

(d)

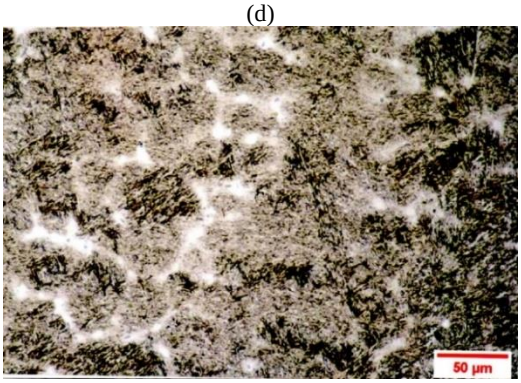

(e)

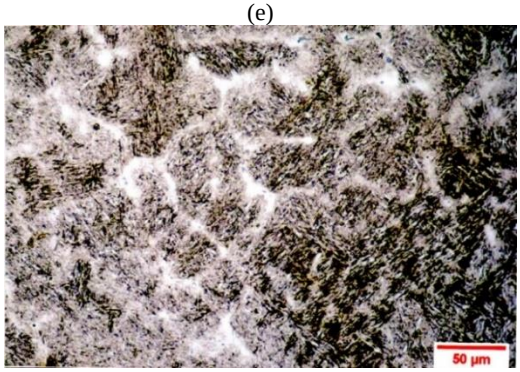

(f)

Figure 5. Microstructure result (a) BNU, (b) BNO, (c) BNM, (d) BNTiU, (e) BNTiO, and (f) BNTiM

only 0.147 wt% Ti being formed in the welded layer based on the OES result. Zhou et al. [16] have reported 0.28 wt%Ti could change the microstructure. When the

Ti composition of Ti raised to 1.17 wt%, the microstructure significantly changed.

From Figures 5(a) and 5(d), we can see a un uniform distribution of ferrite (white region) and martensite (dark area). This behavior was confirmed with the XRD result, where 81.24 wt % ferrite and 15.99 wt % martensite were in the BNU. Moreover, 60.35 wt % ferrite and 32.30 wt % martensite were realized in the BNTiU. The distribution and compositions formed between martensite and ferrite could avoid cracking [32]. It has been no cracking seen in the samples based on microstructure observation.

Quenching in palm oil and engine oil significantly influences the microstructure, similar to other cases reported in literature [20]. Figure 5 shows the martensitic phase and perfect agreement with different research results [33]. Quenching the samples in the solution led to uniformly changing ferrite (α-Fe) distribution between martensite (α'-Fe). Randomly martensite structure is distributed in a ferrite matrix after quenching [34]. This phenomenon is due to the oil's rapid cooling; hence, conducted ferrite becomes finer and does not grow more [35]. The quench heat treatment would be resulting smooth distribution of ferrite and martensite [36].

3. 4. Macrostructure The samples were compared to evaluate the effect of the quenching solution and Ti addition to the macrostructure. Macrostructure observation with a digital camera is shown in Figure 6.

Based on Figure 6, we can see different macrostructures were formed. Fusion between the base metal and weld metal is shown for various samples.

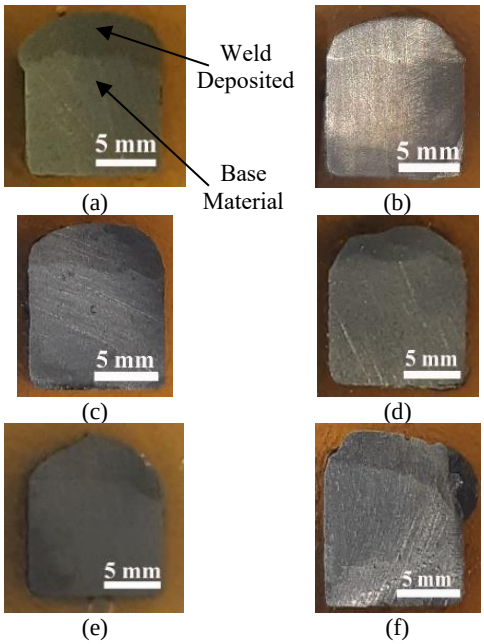

Figure 6. Macrostructure result (a) BNU, (b) BNO, (c) BNM, (d) BNTiU, (e) BNTiO, and (f) BNTiM

There are no visible cracks on the macrostructure. Commonly, this occurs influenced by welding conditions, mechanical restraint, and hydrogen trapping [37, 38]. It means the welding condition in this research could avoid this, and no hydrogen trapping appears in the weld metal.

The penetration of the weld layer would increase by raising the current of welding. Shukla et al. [39] showed 1.2 mm deep penetration when welding using 90 A and positive polarity. Rising to 120 A, reach a deep penetration of around 1.75 mm. The negative polarity and 90º of the electrode angle with a current at 120 A revealed full penetration because of more heat to the weld region [35, 39]. Moreover, a higher current for positive polarity is needed to get full penetration than negative polarity [40]. Plate thickness also influences penetration. Shifting to more thicknesses could increase penetration [35]. In this research, a single layer of weld penetrates approximately 3 mm for various samples. It shows perfect agglomeration between the base material and weld metal. Adding Ti in the weld layer is not influence the penetration. This result differs from others because welding parameters such as an electrode, current, and electrode are different. Commonly penetration of the weld layer is affected by the polarity, current, and angle of the electrode for the SMAW process [39].

3. 5. Hardness Distributions A comparison of the sample hardness was carried out in Figure 7.

Many factors influence hardness were formed. Khamari et al. [35] found that increasing the current would increase the hardness. Dauda et al. [20] found various oil for quenching media resulting in differences in hardness. An exhibit of a fine dispersion of small particles of ferrite and martensite also contributed to higher hardness [20].

Based on Figure 7, we can see that quenching the sample increased the hardness. BNU sample was resulting an average hardness of 503.48 HV. This hardness agrees with the manufacturer of a diverse range of advanced welding consumable HV 600 for single-layer welding, resulting in hardness between 440 – 540 HV [41]. Quench the sample into oils significantly increase the hardness [20].

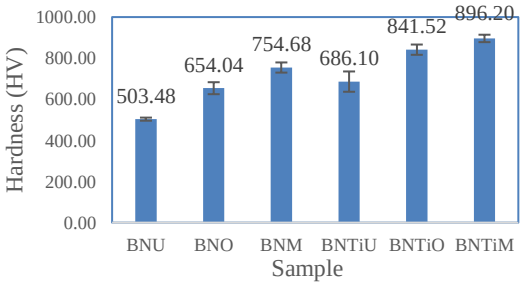

Figure 7. Hardness Vickers of the different specimens

Its seem samples where quenching in oils has higher hardness than air cooling. Air and oil cooling could increase the hardness by around 4.5% and 40%, respectively [42]. Sample where quenching in palm oil has a higher hardness than engine oil. This value is attributed to palm oil having less viscosity than engine oil and thus affecting the higher cooling rate. As we know, engine oil has 64.4 and vegetable oil has 71.9 K/s of viscosity at 40º C [20, 21]. A shift to a higher cooling rate led to higher hardness [43]. For this study, we found that palm oil is the best quenching solution to increase the hardness.

Adding Ti also increases the hardness of the sample when quenching in a different solution. This result perfectly agrees with other research where adding Ti improves the hardness, whereas adding 0.63 wt% Ti could increase the hardness from 56 to 61 HRC [16]. Increasing the Ti from 0.63 to 1.17 wt% could decrease the hardness because too much carbon is consumed when titanium content is 1.17 wt% [16]. Therefore, there is a limitation contained in the layer when Ti is added. Moreover, 0.147 wt% Ti in the weld layer increases hardness by around 0.2% for a sample with and without the quenching process.

Based on Table 1, we can realize that the quenched sample with Ti addition in the engine oil and palm oil led to a decrease in the oxide (Fe_3O_4). This phenomenon may be attributed to the solution cooling rate that increased sample hardness. Iron oxide could affect the strength of the material [44].

Compared to Table 1, an increase in the hardness linearly within increase in the ferrite for a sample with Ti addition. Adding Ti could increase in the hardness of the ferrite matrix [45]. The ferrite phase is the main factor in increasing the hardness in this research. A shift to higher ferrite composition (see Table 1) and fine dispersion of small ferrite particles could enhance the hardness.

Based on the hardness test result, BNTiO, and BNTiM have more hardness than the HSS commercial for a lathe-cutting tool [2]. This value means the samples are recommended for the cutting tool. But this needs deep further investigation.

4. CONCLUSIONS

The effect of Ti addition and quenching of the samples is summarized as follows:

1. Adding titanium (Ti) to the weld layer and quenching the samples after welding in the solution enhances the hardness. This phenomenon is attributed to different phase compositions, oxides, and microstructures.
2. A fine dispersion of small ferrite particles and oxide amount is important in increasing the hardness.
3. Adding Ti in the weld layer did not influence the penetration. Therefore, there is no cracking in the weld and base metal.
4. BNTiO, and BNTiM samples are recommended for cutting tools.

5. ACKNOWLEDGMENT

This research was funded by Engineering Faculty, Universitas Negeri Jakarta (Contract No. 017/UN39.5.FT/PP/IV/2022).

5. REFERENCES

1. Jesudass Thomas, S., and Kalaichelvan, K. "Comparative study of the effect of surface texturing on cutting tool in dry cutting." ***Materials and Manufacturing Processes***, Vol. 33, No. 6, (2018), 683-694. https://doi.org/10.1080/10426914.2017.1376070
2. Susetyo, F. B., Dwiyati, S. T., and Hutomo, M. B. P. "Fabrikasi Lapisan Pada Baja 0 , 192 % C Sebagai Alternatif Pahat Bubut." ***Jurnal kajian Teknik Mesin***, Vol. 5, No. 1, (2020), 42-47.
3. Asad, S., Dilawary, A., Motallebzadeh, A., Atar, E., and Cimenoglu, H. "Influence of Mo on the high temperature wear performance of NiCrBSi hardfacings." ***Tribology International***, Vol. 127, (2018), 288-295. https://doi.org/10.1016/j.triboint.2018.06.022
4. Wang, Y., Gou, J., Chu, R., Zhen, D., and Liu, S. "The effect of nano-additives containing rare earth oxides on sliding wear behavior of high chromium cast iron hardfacing alloys." ***Tribology International***, Vol. 103, (2016), 102-112. https://doi.org/10.1016/j.triboint.2016.06.041
5. Jabbar Hassan, A., Boukharouba, T., Miroud, D., Titouche, N., and Ramtani, S. "Experimental investigation of friction pressure influence on the characterizations of friction welding joint for aisi 316." ***International Journal of Engineering Transactions C: Aspects***, Vol. 33, No. 12, (2020), 2514-2520. https://doi.org/10.5829/ije.2020.33.12c.12
6. Chaidemenopoulos, N. G., Psyllaki, P. P., Pavlidou, E., and Vourlias, G. "Aspects on carbides transformations of Fe-based hardfacing deposits." ***Surface and Coatings Technology***, Vol. 357, (2019), 651-661. https://doi.org/10.1016/j.surfcoat.2018.10.061
7. Yang, K., Gao, Y., Yang, K., Bao, Y., and Jiang, Y. "Microstructure and wear resistance of Fe-Cr13-C-Nb hardfacing alloy with Ti addition." ***Wear***, Vol. 376-377, , (2017), 1091-1096. https://doi.org/10.1016/j.wear.2016.12.062
8. Kesavan, D., and Kamaraj, M. "Influence of aging treatment on microstructure, wear and corrosion behavior of a nickel base hardfaced coating." ***Wear***, Vol. 272, No. 1, (2011), 7-17. https://doi.org/10.1016/j.wear.2011.05.041
9. Wang, H., and Yu, S. "Influence of heat treatment on microstructure and sliding wear resistance of high chromium cast iron electroslag hardfacing layer." ***Surface & Coatings Technology***, Vol. 319, (2017), 182-190. https://doi.org/10.1016/j.surfcoat.2017.04.013
10. Sadeghi, F., Naja, H., and Abbasi, A. "Technology The effect of Ta substitution for Nb on the microstructure and wear resistance of an Fe-Cr-C hardfacing alloy." ***Surface & Coatings Technology***, Vol. 324, (2017), 85-91. https://doi.org/10.1016/j.surfcoat.2017.05.067

11. Singh, H. "Studies the Effect of Iron Based Hardfacing Electrodes on Stainless Steel Properties Using Shielded Metal Arc Welding Process." ***International Journal of Research in Advent Technology***, Vol. 2, No. 4, (2014), 2321-963.
12. Deng, H., Shi, H., and Tsuruoka, S. "Influence of coating thickness and temperature on mechanical properties of steel deposited with Co-based alloy hardfacing coating." ***Surface and Coatings Technology***, Vol. 204, No. 23, (2010), 3927-3934. https://doi.org/10.1016/j.surfcoat.2010.05.013
13. Tavoosi, M., Arjmand, S., and Adelimoghaddam, B. "Surface & Coatings Technology Surface alloying of commercially pure titanium with aluminium and nitrogen using GTAW processing." ***Surface & Coatings Technology***, Vol. 311, (2017), 314-320. https://doi.org/10.1016/j.surfcoat.2016.12.115
14. Ebrahimi, N., Hosseinzadeh, A. S. A., Vaezi, M., and Mozafari, M. "Evaluation of Corrosion Resistance of Bi-layered Plasma-sprayed Coating on Titanium Implants." ***International Journal of Engineering, Transactions A: Basics***, Vol. 35, No. 4, (2022), 635-643. https://doi.org/10.5829/ije.2022.35.04a.03
15. More, S. R., Bhatt, D. V., Menghani, J. V., Paul, C. P., and Desale, G. R. "Laser cladding of pac 718, tribaloy T-700 and METCO 41 C hard facing powders on AISI SS 304L substrate." ***International Journal of Engineering, Transactions B: Applications***, Vol. 34, No. 2, (2021), 480-486. https://doi.org/10.5829/IJE.2021.34.02B.20
16. Zhou, Y. F., Yang, Y. L., Li, D., Yang, J., Jiang, Y. W., Ren, X. J., and Yang, Q. X. "Effect of titanium content on microstructure and wear resistance of Fe-Cr-C hardfacing layers." ***Welding Journal***, Vol. 91, No. 8, (2012), 229-236.
17. Yung, D., Zikin, A., Hussainova, I., Danninger, H., Badisch, E., and Gavrilovic, A. "Tribological performances of ZrC-Ni and TiC-Ni cermet reinforced PTA hardfacings at elevated temperatures." ***Surface and Coatings Technology***, Vol. 309, , (2017), 497-505. https://doi.org/10.1016/j.surfcoat.2016.11.099
18. Faria, D., Brito, P., Ramos, P. A., Resende, L. P., and Ant, D. "Experimental investigation of cooling behavior and residual stresses for quenching with vegetable oils at different bath temperatures." ***Journal of Cleaner Production***, Vol. 216, (2019), 230-238. https://doi.org/10.1016/j.jclepro.2019.01.194
19. Mohmmed, A. A., N Y, Z., and J H, M. "The effect of polymeric quenching media on mechanical properties of medium carbon steel." In IOP Conf. Series: Materials Science and Engineering 1-6. https://doi.org/10.1088/1757-899X/454/1/012053
20. Dauda, M., Kuburi, L. S., and Obada, D. O. "Effects of Various Quenching Media On Mechanical Properties of Annealed 0.509Wt%C -0.178Wt%Mn Steel." ***Nigerian Journal of Technology***, Vol. 34, No. 3, (2015), 506-512.
21. Totten, G. E., Tensi, H. M., and Lainer, K. "Performance of vegetable oils as a cooling medium in comparison to a standard mineral oil." ***Journal of Materials Engineering and Performance***, Vol. 8, No. 4, (1999), 409-416. https://doi.org/10.1361/105994999770346693
22. Dodo, R. M., Ause, T., Shehu, U., Abdulhamid, S., and Onoja, K. K. "Study Of Maize Starch Solution As Quenching Media For 0 62 % C High Carbon Steel." ***International Journal of Engineering***, Vol. XV, No. 4, (2017), 63-68.
23. García-García, V., Mejía, I., and Reyes-Calderón, F. "Experimental and FEM study of Ti-containing TWIP steel weldability." ***Journal of Materials Processing Technology***, Vol. 261, (2018), 107-122. https://doi.org/10.1016/j.jmatprotec.2018.05.028
24. Larson, A. C., and Dreele, R. B. Von. General Structure Analysis System (GSAS) (Vol. 748).
25. Ikubanni, P. P., Agboola, O. O., Adediran, A. A., and Adeleke, A. A. "Experimental data on mechanical properties evaluation of medium carbon steel quenched in different waste media." ***Data in Brief***, Vol. 20, (2018), 1224-1228. https://doi.org/10.1016/j.dib.2018.08.185
26. Tomota, Y., Wang, Y. X., Ohmura, T., Sekido, N., Harjo, S., Kawasaki, T., Gong, W., and Taniyama, A. "In situ neutron diffraction study on ferrite and pearlite transformations for a 1.5Mn-1.5Si-0.2C steel." ***ISIJ International***, Vol. 58, No. 11, (2018), 2125-2132. https://doi.org/10.2355/isijinternational.ISIJINT-2018-336
27. Dalshad Omar, H. "Investigation the Structure and Morphology of Iron Metallic by Difference Techniques." ***Journal of Nanotechnology and Advanced Materials,*** Vol. 3, No. 2, (2015), 57-61. Retrieved from http://dx.doi.org/10.12785/jnam/030201
28. Han, R., Li, W., Pan, W., Zhu, M., Zhou, D., and Li, F. S. "1D magnetic materials of Fe3O4 and Fe with high performance of microwave absorption fabricated by electrospinning method." ***Scientific Reports***, Vol. 4, (2014), 1-5. https://doi.org/10.1038/srep07493
29. Zhou, D. S., and Shiflet, G. J. "Ferrite: Cementite crystallography in pearlite." ***Metallurgical Transactions A***, Vol. 23, No. 4, (1992), 1259-1269. https://doi.org/10.1007/BF02665057
30. Balasubramaniam, R., Ramesh Kumar, A. V., and Dillmann, P. "Characterization of rust on ancient Indian iron." ***Current Science***, Vol. 85, No. 11, (2003), 1546-1555.
31. Lawrynowicz, Z. "Bainite Transformation in Experimental Fe-Cr-Mo-V-Ti-C Steel." ***Advance in Materials Sciences***, Vol. 13, No. 2, (2003), 12-18. https://doi.org/10.2478/adms-2013-0005 Z.
32. Brykov, M. N., Petryshynets, I., Džupon, M., Kalinin, Y. A., Efremenko, V. G., Makarenko, N. A., Pimenov, D. Y., and Kováč, F. "Microstructure and properties of heat affected zone in high-carbon steel after welding with fast cooling in water." ***Materials***, Vol. 13, No. 22, (2020), 1-13. https://doi.org/10.3390/ma13225059
33. Srikarun, B., and Muangjunburee, P. "The effect of iron-based hardfacing with chromium powder addition onto low carbon steel." ***Materials Today: Proceedings***, Vol. 5, No. 3, (2018), 9272-9280. https://doi.org/10.1016/j.matpr.2017.10.100
34. Joshua, T. O., Alao, O. A., and Oluyori, R. T. "Effects of Various Quenching Media on the Mechanical Properties of Inter - Critically Annealed 0.267 % C - 0.83 % Mn Steel." ***International Journal of Engineering and Advanced Technology***, Vol. 3, No. 6, (2014), 121-127.
35. Khamari, B. K., Dash, S. S., Karak, S. K., and Biswal, B. B. "Effect of welding parameters on mechanical and microstructural properties of GMAW and SMAW mild steel joints." ***Iron making and Steel making***, Vol. 47, No. 8, (2019), 844-851. https://doi.org/10.1080/03019233.2019.1623592
36. Bello, K. A., Hassan, S. B., Abdulwahab, M., and Shehu, U. "Effect of Ferrite-Martensite Microstructural Evolution on Hardness and Impact Toughness Behaviour of High Martensite Dual Phase Steel." ***Australian Journal of Basic and Applied Sciences***, Vol. 1, No. 4, (2007), 407-414.
37. Zacharia, T. "Dynamic stresses in weld metal hot cracking." ***Welding Journal***, No. July, (1994), 164-172.
38. Gan, L., Huang, F., Zhao, X., Liu, J., and Cheng, Y. F. "Hydrogen trapping and hydrogen induced cracking of welded X100 pipeline steel in H2S environments." ***International Journal of Hydrogen Energy***, Vol. 43, No. 4, (2018), 2293-2306. https://doi.org/10.1016/j.ijhydene.2017.11.155
39. Shukla, A. A., Joshi, V. S., Chel, A., and Shukla, B. A. "Analysis of Shielded metal arc welding parameter on Depth of Penetration on AISI 1020 plates using Response surface methodology." ***Procedia Manufacturing***, Vol. 20, (2018), 239-246. https://doi.org/10.1016/j.promfg.2018.02.035
40. Wu, D., Chen, H., Huang, Y., He, Y., Hu, M., and Chen, S. "Monitoring of weld joint penetration during variable polarity

plasma arc welding based on the keyhole characteristics and PSO-ANFIS." ***Journal of Materials Processing Technology***, Vol. 239, (2017), 113-124. https://doi.org/10.1016/j.jmatprotec.2016.07.021

41. Nikko, S. *Manufacturers of a Diverse Range of Advance Welding Consumables HV 600*.
42. Dewangan, S., Singhal, P., Selvaraj, S. K., Dev, S. J., and Swathish, R. S. "Analysing strength , hardness and grain-structure of 0.2 %-C steel specimens processed through an identical heating period with different continuous transformation rates specimens processed through an identical heating period with different continuous." In ***Materials Research***, 1-14.
43. Chen, Z., Nash, P., and Zhang, Y. "Correlation of Cooling Rate, Microstructure and Hardness of S34MnV Steel." ***Metallurgical and Materials Transactions B: Process Metallurgy and Materials Processing Science***, Vol. 50, No. 4, (2019), 1718-1728. https://doi.org/10.1007/s11663-019-01621-0
44. Huang, Z., Yi, L., and Jiang, T. "Mechanisms of strength decrease in the initial reduction of iron ore oxide pellets." ***Powder Technology***, Vol. 221, (2012), 284-291. https://doi.org/10.1016/j.powtec.2012.01.013
45. Moon, J., Kim, S., Jang, J. il, Lee, J., and Lee, C. "Orowan strengthening effect on the nanoindentation hardness of the ferrite matrix in microalloyed steels." ***Materials Science and Engineering A***, Vol. 487, No. 1-2, (2008), 552-557. https://doi.org/10.1016/j.msea.2007.10.046

Persian Abstract

چکیده

سختی سطح مواد را که معمولاً از طریق تکنیک هارد فاسینگ انجام می شود، افزایش دهید. Hard facing رایج است، به طوری که مواد با خواص بهتر بر روی مواد فله ارزان‌تر رسوب می‌کنند. این کار با افزودن سیم تیتانیوم (Ti) در طول فرآیند جوشکاری، لایه‌های سختی را ساخت. این تحقیق از فولاد کم کربن به عنوان ماده پایه، سیم بهینه Ti با درجه ۱ برای افزودن Ti، و یک الکترود HV 600 با قطر ۳.۲ میلی متر برای فلز پرکننده استفاده کرد. یک جوش تک لایه با SMAW (قطب مثبت و ۹۰ A) انجام شد. نمونه ها به طور مستقیم پس از جوشکاری در محلول دیگری خاموش شدند. خواص لایه جوش به ترتیب فاز، ساختار، ریزساختار، درشت ساختار و سختی با استفاده از طیف‌سنجی انتشار نوری (OES)، پراش اشعه ایکس (XRD)، میکروسکوپ نوری، دوربین دیجیتال و دستگاه سختی مورد بررسی قرار گرفت. افزودن تیتانیوم (Ti) به لایه جوش و کوئنچ کردن نمونه ها پس از جوشکاری در محلول باعث افزایش سختی می شود. این پدیده به ترکیبات فازی، اکسیدها و ریزساختارهای مختلف نسبت داده می شود. پراکندگی ریز ذرات کوچک و مقدار اکسید در افزایش سختی مهم است. هیچ ترک خوردگی در جوش و فلز پایه وجود ندارد. در نتیجه، نمونه‌های BNTiO و BNTiM برای ابزارهای تراشکاری توصیه می‌شوند.